Optical studies on sol–gel derived titanium dioxide films

A.K.Ray, S.M.Tracey, B.McQuillin and S.N.B.Hodgson

Abstract: Optical absorption $A(\lambda)$ and transmission $T(\lambda)$ spectra for normal incidence have been obtained within the wavelength (λ) range 300–900nm for titanium dioxide (TiO_2) films in anatase form prepared by the sol–gel method. The dispersion relation for refractive indices is in agreement with the oscillator model. The refractive index is found to be independent of thickness. Above the absorption tail, optical absorption is believed to be due to nondirect electronic processes involving no transitions between localised states in a single layer thick TiO_2 film. For a multilayered film, transitions between localised states are probable as equal as those between all other states.

1 Introduction

Titanium dioxide (TiO_2) exhibits a range of potentially useful properties such as high refractive index, high dielectric constant and chemical stability. The material exists in three stable crystalline phases: brookite, anatase and rutile. Rutile is known to be the most stable phase. Due to practical importance the materials have attracted much interest in recent years for use in a variety of optical, electrical and optoelectronic applications including antireflectance coatings [1], electrochromic display devices [2] and planar waveguides [3, 4]. The materials can be formulated in thin film form by using sputtering [5], a plasma beam generator [6], chemical vapour deposition [7] and spin coating [8]. TiO_2 thin films can also be prepared in amorphous form, with the anatase form being of particular interest for the rapidly developing areas of electrochemical and solid-state dye sensitised photovoltaic cells [9, 10]. The polycrystalline and amorphous forms of TiO_2 can be readily prepared using the sol–gel technique [11] which offers the possibility of relatively low cost, large-scale production of thin films. Recent work has identified significant interactions between process parameters such as withdrawal rate, sol concentration and the number of coating layers and their effects on structural, optical and electrical properties of sol–gel derived TiO_2 films [12]. This article reports the results of optical measurements on sol–gel derived anatase films on glass substrates. Experimental data were analysed to determine the film thickness and refractive indices and to provide an interpretation of the electronic transition processes involved in optical absorption. The nature of interband transitions was not investigated in earlier studies and the present investigations now show that nondirect transitions are responsible for optical absorption. An electronic band structure is proposed for a polycrystalline TiO_2 film. Sol–gel derived TiO_2 films are normally used in dye-sensitised photoconductive cells [13, 14] and the knowledge of band properties is important for understanding the mechanism of charge transfer from the dye molecule to the oxide film.

IEE Proceedings online no. 20000698

DOI: 10.1049/ip-smt:20000698

Paper first received 8th October 1999 and in revised form 2000

A.K. Ray, S.M. Tracey and B. McQuillin are with the Physical Electronics & Fibre Optics Research Laboratories, School of Engineering, Sheffield Hallam University, Pond Street, Sheffield S1 1WB, UK

S.N.B. Hodgson is with the Institute of Polymer Technology and Materials Engineering, Loughborough University, Loughborough, Leicestershire LE11 3TU UK

2 Experimental techniques

Chemically and thermally stable films of titanium dioxide were prepared using the sol–gel method. A solution was prepared by mixing 5.04ml glacial acetic acid CH_3COOH (Aldrich 99.5%) and 50ml anhydrous ethanol (Aldrich 99.7–100%) for 5 min and then 6.3ml titanium (IV) isopropoxide $Ti[OCH(CH_3)_2]_4$ (97% pure) was added to this solution. An additional period of 2 min was allowed for proper blending and dip coating was then carried out onto ultrasonically cleaned glass substrate under atmospheric conditions. The addition of acetic acid is necessary as a reaction-modifying agent to prevent the rapid and uncontrolled hydrolysis of the titanium alkoxide which otherwise forms particulate reaction products rather than gels suitable for dip coating. During the dipping process, the substrates were generally withdrawn with a speed of 250mm/min but different speeds were also used for comparative studies. The samples were allowed to dry in air for 24h and subsequently heat treated at a temperature of 500°C for 5h. Heat treatment at temperatures higher than 500°C was not investigated due to the limitations of the glass substrates used. Using a Phillips PW 1710 diffractometer with monochromatic Cu radiation and a scan speed of 0.01 degree (2θ) per second, X-ray diffraction studies were performed on residues of the sol mixture, which had been previously dried and then subjected to the same heat treatment as for the dip-coated films. Optical transmission and absorption spectra for the heat-treated TiO_2 films were investigated using an ATI Unicam UV/visible spectrophotometer. The thickness of the films was also independently measured using a planar surfometer (Surfcom 300) with a stated accuracy of $\pm 0.01\mu m$. The stylus was made to traverse across the substrate up to the coating edge and beyond for a total distance of 2mm. For the purpose of electrical measurements, the TiO_2 film was dip-coated on an $InSnO_2$ substrate and gold was evaporated as a top electrode. All experiments were repeated and good reproducibility of the results was achieved.

3 Results and discussions

Fig. 1 shows a typical powder X-ray diffraction pattern obtained from sol residues heated at 500°C for 5h. Using Bragg's law, values of interplanar spacing distance for each peak were calculated. The results of calculations are summarised in Table 1 and they correspond well to data for anatase TiO_2 film. The rutile and brookite forms of TiO_2 were not observed during these investigations. The amorphous phase of TiO_2 film was obtained from the sols that were not affected by heat treatment. For comparison, the analysis of diffraction patterns for films manufactured under identical conditions, but heated to 350°C for the same length of time, does not produce similar results. The pattern in Fig. 1*b* shows the form of TiO_2 film to be predominantly amorphous with the appearance of two peaks corresponding to interplanar distances of 35.37nm and 30.86nm at angles of ≈25° and ≈27°. It is therefore believed that the heat treatment temperature at 500°C caused a gradual crystallisation of the material to the anatase structure.

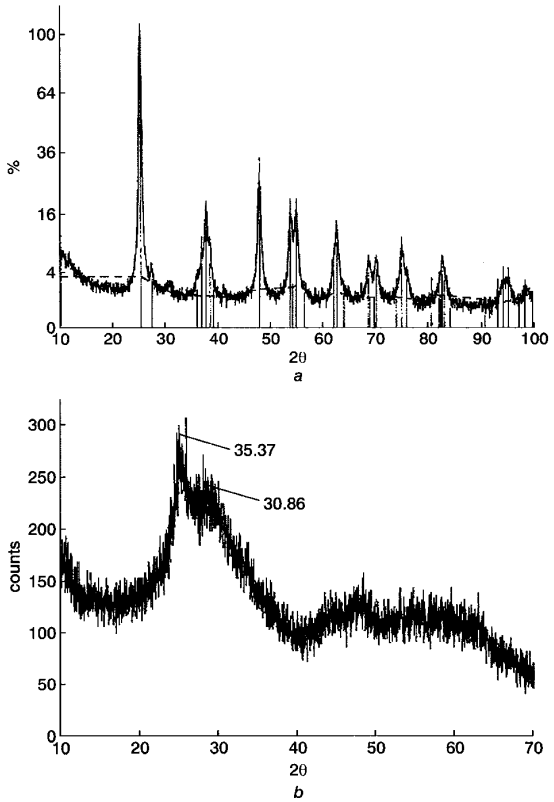

Fig. 1 *Effect of heat treatment on the X-ray diffraction patterns of TiO_2 sol–gel residues for a gel heated to 500°C and 350°C*
a 500°C
b 350°C

Fig. 2 shows typical transmission spectra for the bare glass substrate and also substrates coated with three different layers of TiO_2 films. The spectra were corrected for the effects of optical absorption in the substrates. As expected, films exhibit a significantly large fraction of transmission for the range of wavelengths 350nm ≤ λ ≤ 900nm. The appearance of interference fringes in the transmission spectra is caused by multiple reflections at the boundary of the film and the substrate. The number of maxima and minima in interference patterns increases with that of the layers. Interference patterns were found to disappear for samples coated with less than four layers. Using the condition for interference for two adjacent maxima (or minima) at wavelengths λ_1 and λ_2, the thickness d of the TiO_2 films is determined from the standard expression

$$d = \frac{\lambda_1 \lambda_2}{2[\lambda_1 \mu(\lambda_2) - \lambda_2 \mu(\lambda_1)]} \quad (1)$$

where $\mu(\lambda_1)$ and $\mu(\lambda_2)$ are the refractive indices of the TiO_2 film for λ_1 and λ_2, respectively.

Table 1: Measured values (a) and reference data (b) obtained for an anatase film from Philips PC-APD software for interplanar spacing

Peak number	Angle (°) at which the peak is positioned		Values of interplanar spacing, nm	
	(*a*)	(*b*)	(*a*)	(*b*)
1	25.38	25.281	35.065	35.2
2	37.78	37.801	23.793	23.78
3	48.03	48.05	18.927	18.92
4	53.83	53.891	17.017	16.999
5	55.215	55.062	16.622	16.665
6	62.79	62.69	14.787	14.808
7	68.725	68.762	13.647	13.641
8	70.255	70.311	13.387	13.378
9	75.075	75.032	12.643	12.649
10	82.7	82.662	11.66	11.664

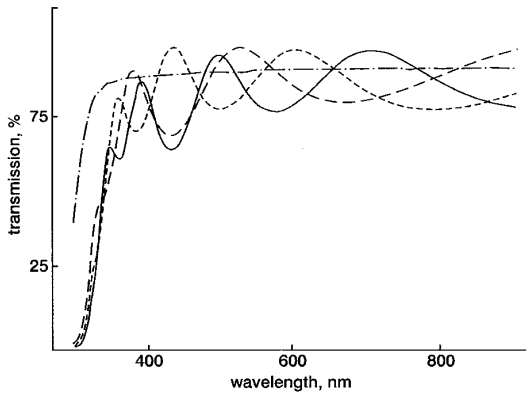

Fig. 2 *Transmission interference fringes observed for five-, six- and seven-layer thick TiO_2 films*
Transmission spectrum T_s for the glass substrate is also shown, withdrawal rate of 250mm/min
– – – – five layers
– – – – six layers
——— seven layers
— – — T_s

The method due to Swanepoel is employed to estimate the refractive indices $\mu(\lambda)$ [15]. If $\mu_s(\lambda)$ is the refractive index of the substrate, $\mu(\lambda)$ for the film can be found according to the formula

$$\mu(\lambda) = \left[M + \sqrt{(M^2 - \mu_s^2)}\right]^{1/2} \quad (2)$$

where M is given for a wavelength λ in the form

$$M = \frac{\mu_s^2 + 1}{2} + 2\mu_s \frac{T_{max}(\lambda) - T_{min}(\lambda)}{T_{max}(\lambda) T_{min}(\lambda)} \quad (3)$$

$T_{max}(\lambda)$ and $T_{min}(\lambda)$ lie on the two curves enveloping the maxima and minima of the interference patterns. The refractive index $\mu_s(\lambda)$ is calculated from the transmission spectrum $T_s(\lambda)$ for the glass substrate using the expression of

$$\mu_s(\lambda) = \frac{1}{T_s} + \sqrt{\frac{1}{T_s^2} - 1} \qquad (4)$$

A selfconsistent iterative procedure was developed to solve eqns. 1–4. The refractive index profile $\mu(\lambda)$ within the transmission regime and the thickness of the TiO_2 film were calculated from the solutions. Parabolic interpolation between the three nearest experimental points is adopted to determine intermediate values of $T_{max}(\lambda)$ and $T_{min}(\lambda)$. Similar experiments were also carried out on films produced with a withdrawal rate of 100mm/min.

Fig. 3 shows an approximately linear correlation between the number of applications and the overall coating thickness for both withdrawal rates of 250mm/min and 100mm/min. As expected, films produced by a fast withdrawal rate are found to be thicker than those produced by a slow rate. Results obtained from the surface profile experiments show a reasonable degree of consistency between the two sets of data obtained from independent measurements.

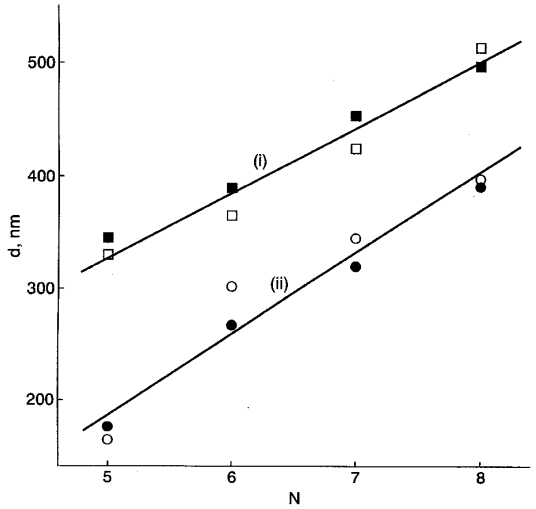

Fig. 3 *Set of two linear graphs showing the relationship between the thickness of TiO_2 film and the number of applications for withdrawal rate of (i) 250mm/min and (ii) 100mm/min*
Open and closed symbols identify the data obtained from the Swanepoel method and the surface profiling measurements, respectively

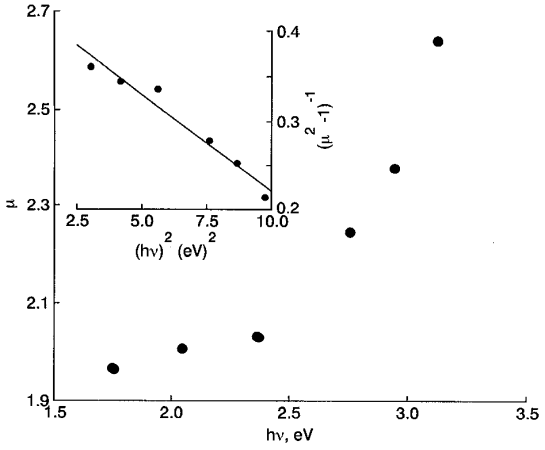

Fig. 4 *Curve showing the variation of refractive index μ with incident photon energy $h\nu$ for a seven layer thick TiO_2 film*
Plot of $(\mu^2 - 1)^{-1}$ against $h\nu^2$ is given in the inset

As shown in Fig. 4, refractive indices of a seven-layer thick TiO_2 film are found to decrease with the wavelength. This observation is consistent with results reported earlier [10]. Using the least-squares technique, a linear fit is obtained in the inset for the dependence of $(\mu^2 - 1)^{-1}$ on the square of photon energy ($h\nu$). This implies that the dispersion relation can be explained in terms of the single oscillator model given in the form [16]

$$\mu = \left[1 + \frac{E_d E_s}{E_s - h^2\nu^2}\right]^{1/2} \qquad (5)$$

Values of the single effective oscillator energy E_d and the dispersion energy E_s are estimated to be 2.2eV and 16.5eV from the zero energy intercept and the slope of the graph, respectively. The average oscillator strength S is estimated to be $23 \times 10^{12}m^{-2}$ from the relationship of $S = E_d E_s/(h^2c^2)$. Similar analysis was performed for the remaining layers and also for the samples prepared with the withdrawal speed of 100mm/min. It is found that refractive indices show a weak dependence on the film thickness within the range considered.

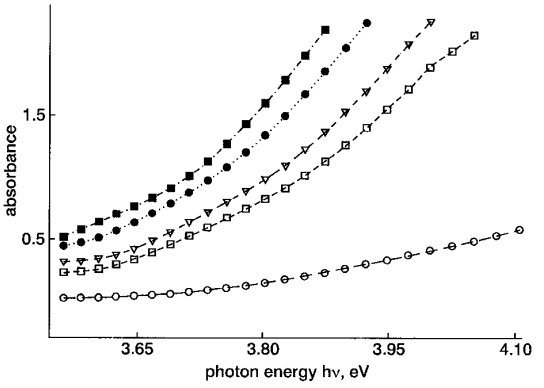

Fig. 5 *Absorption spectra for TiO_2 film with five different thickness in the range of photon energy 3.5–4.1eV*
○–○ one layer
□–□ five layers
▽–▽ six layers
●–● seven layers
■–■ eight layers

Fig. 5 displays the absorbance as a function of incident photon energy ($h\nu$) in the range 3.5–4.1eV for a variety of coating layers. Absorption edges are not expected to be sharp because of random orientation of crystallites within the region on which the incident beam is focused. It is to be noted that the absorption edge decreases to a lower energy for a multilayered sample than that for a single-layered film. The energy-dependence of the absorbance A is usually written in the form [17]

$$A(h\nu) = \left(\frac{Bd}{h\nu}\right)(h\nu - E_0)^n \qquad (6)$$

where the optical band gap E_0 defines the energy position of the optical absorption edge and the power index n describes the nature of electronic transitions. B depends upon the minimum metallic conductivity σ_0, refractive index μ, the width of band edges ΔE and the nature of electronic transition n. Eqn. 6 is valid for the present investigation since the absorption coefficient is found to be greater than $10^4 m^{-1}$ for all layers.

Eqn. 6 can be rewritten in the form [18]

$$Y/Y' = \frac{h\nu - E_0}{n} \qquad (7)$$

where $Y = A(h\nu)h\nu$ and

$$Y' = \frac{d[A(h\nu)h\nu]}{d(h\nu)}$$

The midpoint difference rule is employed to compute the derivative $d[A(h\nu)h\nu]/d(h\nu)$ from the experimental data of Fig. 5. The advantage of using eqn. 7 is that there is no requirement of prior knowledge of the film thickness.

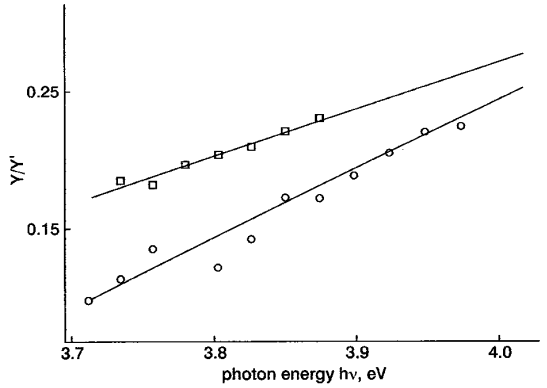

Fig. 6 *Two graphs showing linear dependence of Y/Y' on incident photon energy hv in the range of 3.7–4.0eV for an eight-layer thick TiO_2 film*
□ eight layers
○ one layer

Fig. 6 shows the linear plots of Y/Y' as a function of $h\nu$ for photon energies greater than the absorption edge for one- and eight-layered thick films. Values of n and E_0 are determined from the gradient and intercept, respectively. E_0 takes on values of 3.6eV and 3.3eV for single and eight-layered films, respectively. Similar analysis was performed for the remaining layers. It is found that the value of E_0 is independent of the number of coatings in a multilayered film and this observation agrees well with the plots in Fig. 5. The value of n for a single layer is also different from that of multilayers. These data may be interpreted in terms of the model due to Mott and Davis [19] for nondirect transitions involving the energy supply by incident photons and no emission or absorption of phonons. The value of $n = 2$ for a single layer implies that the probability of transitions between localised states is small. However, for $n = 3$ in the case of a multilayered TiO_2 film, transitions between localised states become equally probable in a multilayered system as those involving the continuum states. This is a feasible observation since the density of states localised at the interface between consecutive layers is large. In both cases, the density of states at the band edges is expected to be linear with energy, and the width of band edges may be derived from the relation [19]

$$\Delta E = \left(\frac{4\pi\sigma_0}{3\mu cB}\right)^{1/2} \quad (8)$$

where the velocity of light c is taken to be $3.0 \times 10^8 ms^{-1}$.

σ_0 is found to be $3.8 \times 10^{-4} Sm^{-1}$ from the Arrhenius plot of conductivity of a 0.36μm TiO_2 film as a function of the inverse of temperature T (Fig. 7). B is assumed to be constant in the optical frequency range and ΔE is found to lie within the range of 0.1–0.2eV. The electronic band gap $E_C - E_V$ is, therefore, estimated to be 3.6eV for a multilayered film.

4 Concluding remarks

It is found that sol–gel derived TiO_2 films possess a relatively high refractive index with its typical value of 2 at 500nm. Vorotilov *et al.* [20] determined an index of 2 for anatase, which is in agreement with the present data. The refractive index of TiO_2 thin films prepared by ion beam assisted deposition methods lies between 2.3 and 2.7 [21].

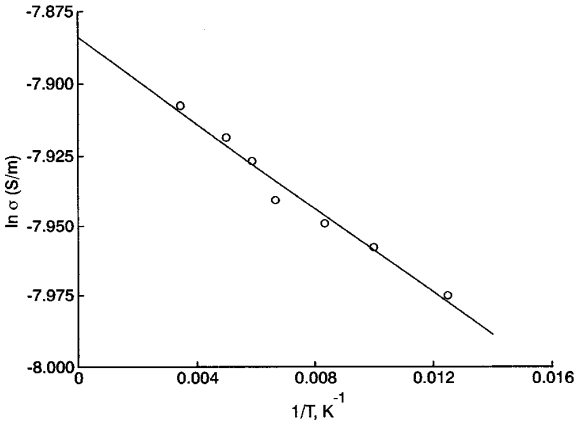

Fig. 7 *Variation of conductivity σ with reciprocal temperature for TiO_2 film*

Values of the optical band gap E_0 are comparable to those previously reported for TiO_2 films. Values of E_0 are found to be 3.2eV and 3.0eV for reactively triode sputtered TiO_2 films in anatase and rutile, respectively [22]. Leinen *et al.* [23] have recently reported a band gap in the range of 3.3–3.42eV for induced chemical vapour deposited anatase films. Fresnel loss occurs at the interface between the substrate and the first layer due to the mismatch in their refractive indices. It is also reported that sodium atoms diffuse into TiO_2 film from the glass substrate [24]. This diffusion process is likely to cause the changes in optical properties of the single-layer film but no evidence of strong sodium contamination was, however, observed from the diffraction pattern for a single layer in the present studies. Both Fresnel and diffusion effects become less important for the subsequent coating of layers.

5 Acknowledgments

The authors are grateful to Dr A. Hassan of Sheffield Hallam University and Professor C.A. Hogarth of Brunel University for fruitful discussions. S.M. Tracey is grateful to Sheffield Hallam University for the award of a research studentship.

6 References

1 VANBOMMEL, , and BERNARDS, T.N.M.: 'Spin coating of titanium ethoxide solutions', *J. Sol-Gel Sci. Technol.*, 1997, **8**, (1–3), pp. 459–463
2 CANTAO, M.P., CISNEROS, J.L., and TORRESI, R.M.: 'Electrochromic behavior of sputtered titanium-oxide thin-films', *Thin Solid Films.*, 1995, **259**, pp. 70–74
3 YOSHIDA, M., LAL, M., KUMAR, N.D., and PRASAD, P.N.: 'TiO_2 nano-particle-dispersed polyimide composite optical waveguide materials through reverse micelles', *J. Mater. Sci.*, 1997, **32**, (15), pp. 4047–4051
4 SOREK, Y., REISFELD, R., FINKELSTEIN, I., and RUSCHIN, S.: 'Sol-gel glass waveguides prepared at low-temperature', *Appl. Phys. Lett.*, 1993, **63**, (24), pp. 3256–3258
5 WEINBERGER, B.R., and GARBER, R.B.: 'Titanium dioxide photocatalysts produced by reactive magnetron sputtering', *Appl. Phys. Lett.*, 1995, **66**, (18), pp. 2409–2411
6 HA, H., MOON, B.K., HORIUCHI, T., INSUSHIMA, T., ISHIWARA, H., and KONINUMA, H.: 'Structure and electric properties of TiO_2 films prepared by cold plasma torch under atmospheric pressure', *Mater. Sci. Technol.*, 1996, **B41**, pp. 143–147
7 LEE, W.G., WOO, S.I., KIM, J.C., CHOI, S.H., and OH, K.H.: 'Preparation and properties of amorphous TiO_2 thin films by plasma enhanced chemical vapour deposition', *Thin Solid Films*, 1994, **237**, pp. 105–111
8 KIM, Y.J., and FRANCIS, L.F.: 'Processing and characterisation of porous TiO_2 coatings', *J. Am. Ceram. Soc.*, 1993, **76**, (3), pp. 737–742
9 BACH, U., LUPO, D., COMTE, P., MOSER, J.E., WEISSOORTEL, F., SALBECK, J., SPREITZER, H., and GRATZEL, M.: 'Solid-state dye-sensitized mesoporous TiO_2 solar cells with high photon-to-electron conversion efficiencies', *Nature*, 1998, **395**, pp. 583–585

10 TRACEY, S.M., RAY, A.K., and SHISHIYANU, T.S.: 'Device characteristics of CuPc/TiO_2 heterojunctions', *IEE Proc. Circuits Devices Syst.,* 1998, **145**, (3), pp. 383–387
11 TRACEY, S.M., HODGSON, S.N.B., RAY, A.K., and GHASSEMLOOY, Z.: 'The role and interactions of the process parameters on the nature of alkoxide derived sol–gel films', *J. Mater. Process. Technol.,* 1998, **7**, pp. 86–94
12 SELVARAJ, U., PRASADARAO, A.V., KOMARNENI, S., and ROY, R.: 'Sol-gel fabrication of epitaxial and oriented thin films', *J. Am. Ceram. Soc.,* 1992, **75**, (5), pp. 1167–1170
13 O'REGAN, B., and GRATZEL, M.: 'A low-cost, high-efficiency solar cell based upon dye-sensitised colloidal TiO_2 films', *Nature,* 1991, **353**, pp. 737–740
14 KRUGER, J., BACH, U., and GRATZEL, M.: 'Modification of TiO_2 heterojunctions with benzoic acid derivatives in hybrid molecular solid-state devices', *Adv. Mater.,* 2000, **12**, (6), pp. 447–451
15 SWANEPOEL, R.: 'Determination of the thickness and optical-constants of amorphous-silicon', *J. Phys. E, Sci. Instrum.,* 1983, **16**, (12), pp. 1214–1222
16 WEMPLE, S.H., and DIDOMENICO, M.: 'Behaviour of the electronic dielectric constant in covalent and ionic materials', *Phys. Rev.,* 1971, **3**, (4), pp. 1338–1351
17 TAUC, J.: 'The optical properties of solids' ABELES, F. (Ed.) (North-Holland Publ. Co. Amsterdam, 1970) p. 277
18 RAY, A.K., and HOGARTH, C.A.: 'On the analysis of experimental data on optical absorption in non-crystalline materials', *J. Phys. D, Appl. Phys.,* 1990, **23**, pp. 458–459
19 MOTT, N.F., and. DAVIS, E.A.: 'Electronic materials in non-crystalline materials' (Claredon Press, 1979) p. 291
20 VOROTILOV, K.A., ORLOVA, E.V., and PETROVSKY, V.I.: 'Sol-gel TiO_2 films on silicon substrates', *Thin Solid Films,* 1992, **207**, pp. 180–184
21 LEINEN, D., FERNANDEZ, A., ESPINOS, J.P., BELDERRAIN, T.R., and GONZALEZ-ELIPE, A.R.: 'Ion-beam-induced chemical-vapour-deposition for the preparation of thin-film oxides', *Thin Solid Films,* 1994, **241**, (1–2), pp. 198–201
22 TANG, H., PRASAD, K., SANJINES, R., SCHMID, P.E., and LEVY, F.: 'Electrical and optical properties of TiO_2 anatase thin films', *J. Appl. Phys.,* 1994, **75**, (4), pp. 2042–2047
23 LEINEN, D., ESPINOS, J.P., FERNANDEZ, A., and GONZALEZ-ELIPE, A.R.: 'Ion-beam-induced chemical-vapor-deposition procedure for the preparation of oxide thin-films 1. Preparation and characterisation of TiO_2 thin-films', *J. Vac. Sci. Technol. A,* 1994, **12**, (5), pp. 2728–2732
24 FERNANDEZ, A., LASSALETTA, G., JIMENEZ, V.M., JUSTO, A., GONZALEZ-ELIPE, A.R., HERRMANN, J.M., TAHIRI, H., and AITCHOU, Y.: 'Preparation and characterisation of TiO_2 photocatalysts supported on various rigid supports (glass, quartz and stainless steel) Comparative studies of photocatalytic activity in water purification', *Appl. Catalysis B - Environ.,* 1995, **7**, (1–2), pp. 49–63